Dissecting Contributions of Prefrontal Cortex and Fusiform Face Area to Face Working Memory

T. Jason Druzgal[1,2] and Mark D'Esposito[1]

Abstract

■ Interactions between prefrontal cortex (PFC) and stimulus-specific visual cortical association areas are hypothesized to mediate visual working memory in behaving monkeys. To clarify the roles for homologous regions in humans, event-related fMRI was used to assess neural activity in PFC and fusiform face area (FFA) of subjects performing a delay-recognition task for faces. In both PFC and FFA, activity increased parametrically with memory load during encoding and maintenance of face stimuli, despite quantitative differences in the magnitude of activation. Moreover, timing differences in PFC and FFA activation during memory encoding and retrieval implied a context dependence in the flow of neural information. These results support existing neurophysiological models of visual working memory developed in the nonhuman primate. ■

INTRODUCTION

In neurophysiological studies of monkeys, visual working memory recruits both prefrontal cortex (PFC) and stimulus-specific inferior temporal cortex (IT). Lesions to either of these regions produce differential impairments in working memory task performance. IT lesions selectively hinder performance on visual working memory tasks involving specific stimulus attributes (i.e., color), whereas PFC lesions cause more global working memory impairment across visual, tactile, and auditory stimuli (for a review, see Fuster, 1997). In single-unit recording studies, PFC activity has been associated with encoding visual stimuli into memory, maintaining that stimulus information across a delay period, and determining whether a probe stimulus matches the stimulus held in memory (e.g., Miller, Erickson, & Desimone, 1996; Fuster & Bauer, 1974). In contrast, IT neurons show greater stimulus selectivity during encoding (Miller, Li, & Desimone, 1993) and maintaining information across a delay period (Nakamura & Kubota, 1995; Miyashita & Chang, 1988; Fuster & Jervey, 1982), but similar information to PFC about the behavioral relevance of a probe stimulus (Miller et al., 1993, 1996). The differences in single-unit activity coupled with the asymmetry in impairments caused by focal lesions suggest that IT and PFC perform different but complementary functions to support visual working memory.

Whether IT and PFC have similar roles in the human is a matter of open debate. Specific controversy surrounds the idea of which brain regions maintain the memory trace during the delay period of a visual working memory task. Despite evidence for a distributed representation of the visual memory trace in monkeys, the majority of human neuroimaging studies have focused on the PFC as the primary locus of the memory trace (for reviews, see D'Esposito, Aguirre, Zarahn, & Ballard, 1998; D'Esposito, Postle, & Rypma, 2000). In the present study, in order to investigate the role of PFC and visual association cortex in working memory, we used event-related fMRI and a delayed item recognition task that varied with the mnemonic load for faces (Figure 1). The event-related design allowed us to separately examine: (1) an encoding period where subjects viewed between one and four faces, (2) a maintenance period where subjects remembered the encoded faces across a short delay, and (3) a retrieval period where subjects gave a motor response indicating if a probe face matched one of the remembered faces. Parametric variations of mnemonic load allowed correlations between fMRI signal and levels of a specific mental process—memory for faces. In parallel to the monkey literature, analyses focused on a functionally defined region of temporal cortex—fusiform face area (FFA; Kanwisher, McDermott, & Chun, 1997; Puce, Allison, Gore, & McCarthy, 1995)—and the PFC. Allowing for methodological differences, activity in human FFA and PFC corresponded well with IT and PFC single-unit data from monkeys. The manipulation of memory load also provided additional insight into the role of FFA and PFC in visual working memory for faces. These results will support a model where PFC biases posterior unimodal association cortical activity in

[1]University of California, Berkeley, [2]University of Pennsylvania

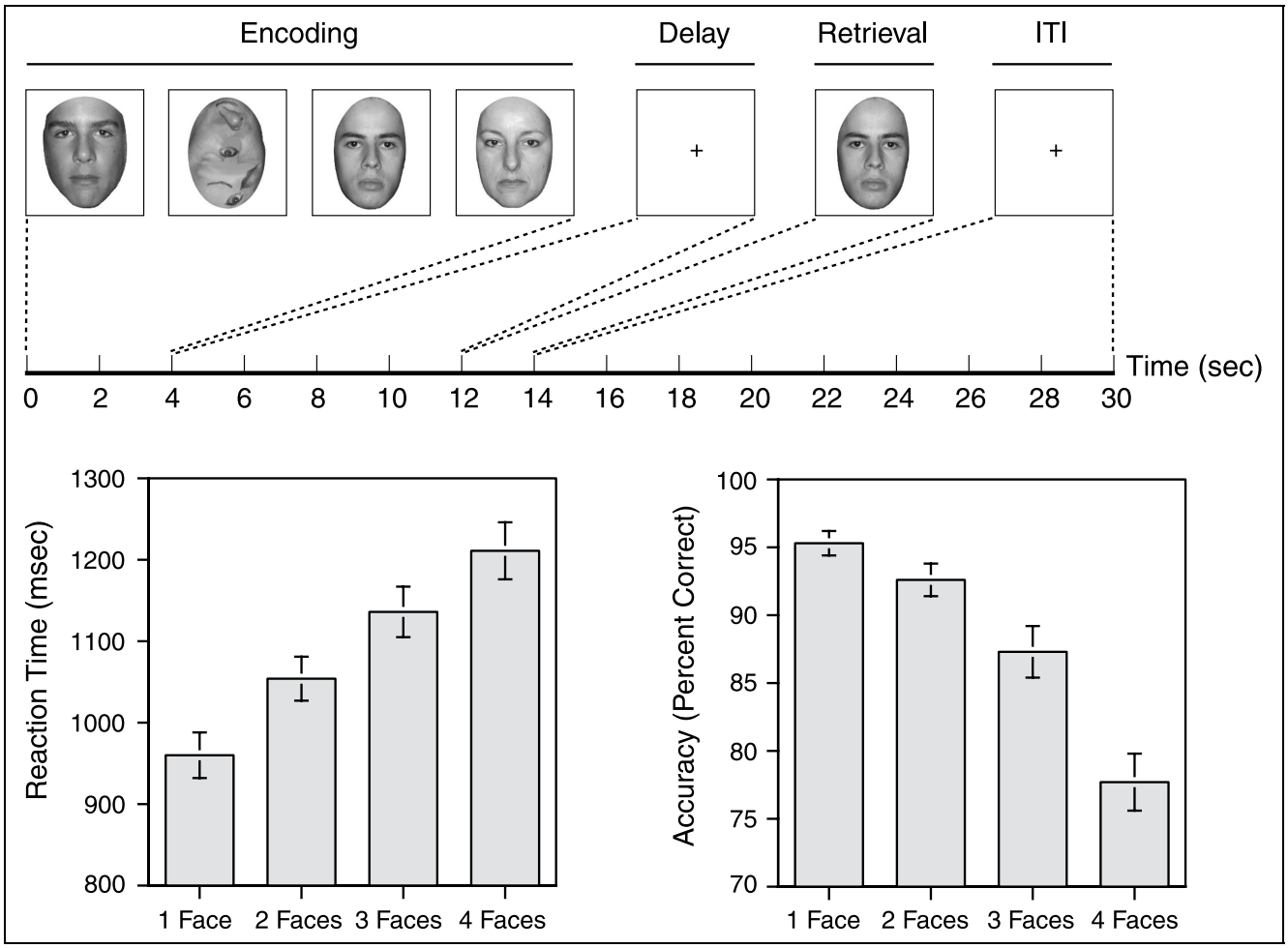

Figure 1. (Top) Schematic of the face delay-recognition task. Each box represents a stimulus display event, and the dotted lines connecting each box to the timeline indicate the duration of each event and its position with respect to collection of fMRI images. Depending on the trial type, the encoding stimulus set contained one, two, three, or four faces, with the remainder of the images being jumbled faces. Only the three-face trial type is shown here. Subjects were asked to remember all of the intact faces during the delay period. Following the delay, a probe face prompted subjects to give a motor response indicating whether the probe matched a face from the stimulus set. (Bottom) Accuracy and reaction time data ($N = 9$) for the face recognition task during scanning.

favor of behaviorally relevant representations necessary for guiding behavior.

RESULTS

Behavioral Data

Behavioral measures included accuracy of response and reaction time for correct trials (Figure 1). All subjects performed significantly above chance (50%) at each mnemonic load, although accuracy declined with increased load. Only trials where subjects gave correct responses were included in the subsequent fMRI analyses. For those trials where subjects responded correctly, reaction time increased linearly (slope = 81 ± 11 msec/face, $p < .0001$; intercept = 898 ± 30 msec, $p < .0001$) with mnemonic load. One subject was excluded from the behavioral analysis due to a hardware problem that prevented the collection of behavioral data. Many subjects did not report a consistent strategy for performing the task, but the two most common were: (1) active mental rehearsal of the face images during the delay, and (2) a gestalt strategy that lacked rehearsal and relied more on stimulus familiarity at recognition. Strategies differed between subjects at the lower mnemonic loads, but most subjects reported a reliance on stimulus familiarity at higher mnemonic loads. It is not possible to determine when subjects were using particular strategies, or whether other strategies might have been utilized.

Imaging Data: Identification of Functional Regions of Interest (ROIs)

The localizer experiment successfully identified a face-selective FFA in all 10 subjects (Figure 2). A bilateral FFA appeared in nine subjects, and one subject had a right-lateralized FFA. The average size of the FFA was 15.3 ± 3.4 voxels (1.08 ± 0.24 cm^3). In the bilateral FFA, the

volume of the right cluster of activation was 11.7 ± 2.6 voxels (0.82 ± 0.18 cm^3), compared with a left cluster volume of 8.1 ± 1.7 voxels (0.57 ± 0.12 cm^3). Similarly, the percent signal change for viewing faces relative to viewing objects was 1.5 ± 0.2% in the right FFA, while the corresponding change was 1.2 ± 0.2% in left FFA. Thus, the FFA was somewhat right-lateralized even in subjects with a bilateral FFA. Our results agree with previous studies finding bilateral FFA activity (Puce et al., 1995) but also support findings that the degree of lateralization might depend strongly on subtle aspects of the control stimuli (Kanwisher et al., 1997). The ROIs used in the subsequent fMRI data analyses were defined as the composite bilateral FFA for each subject.

The localizer experiment was also used to identify an object-selective region of fusiform gyrus (Figure 2), previously called the fusiform object area (FOA; Druzgal & D'Esposito, 2001). In subsequent analyses, the FOA served as a control region for hypotheses that face working memory tasks only recruit stimulus-specific regions of temporal cortex. The FOA was bilateral in all subjects, with a mean size of 28.5 ± 5.2 voxels (2.00 ± 0.37 cm^3). The FOA sat medial to the FFA in axial brain slices, in agreement with previous studies of object-selective temporal regions.

The PFC ROI was bilateral in all subjects, with a mean size of 124 ± 24 voxels (8.72 ± 1.7 cm^3).

Imaging Data: Working Memory Contrast within Functionally Defined ROIs

Trial-averaged changes in fMRI signal across all subjects are shown for PFC, FFA, FOA, and a combination of FFA and FOA (Figure 3). The combination of FFA and FOA represented a broad subset of the voxels within the anatomic fusiform gyrus, in an effort to facilitate comparison to previously published studies that used anatomic ROIs (Jha & McCarthy, 2000). The color spectra in Figure 3 provide a temporal guideline for where to expect changes attributable to separate trial components of encoding, delay, and retrieval periods. Given the sluggishness of the hemodynamic response and individual variability in the hemodynamic response function (HRF; Aguirre, Zarahn, & D'Esposito, 1998b), this visual deconvolution into individual trial components is a rough estimate at best. To quantify the mapping of fMRI signal onto specific trial periods (early encoding, late encoding, delay, and retrieval periods), regression models were used to statistically assess changes in blood oxygenation level dependent (BOLD) response from the four ROIs in individual subjects. Specifically, the analyses examined main effects—changes in fMRI signal relative to the baseline across all mnemonic loads—in each trial period and ROI. Then we tested the same trial periods and ROIs for linear effects—changes in fMRI signal that varied as a linear function of mnemonic load.

PFC activity persisted throughout the trial at all mnemonic loads (Figure 3). For all load levels, fMRI activity peaked during the encoding period, plateaued across the delay period, and peaked again during the retrieval period. As shown in Figure 4A, the main effect of activity across loads was significant during each of the early encoding, late encoding, delay, and retrieval periods. When separated by mnemonic load, activity during the encoding peak and maintenance plateau was greater for the three- and four-face conditions than for one or two faces (Figure 3). These time series suggest that load effects at late encoding and delay might be a step function in the PFC, but statistical evaluation suggested a strong linear component. As shown in Figure 4B, PFC activity increased linearly with mnemonic load during the late encoding and delay periods, but not at early encoding or retrieval.

Although the FFA time series differed from PFC, activity in FFA also persisted throughout the trial at all mnemonic loads (Figure 3). At all loads, FFA activity peaked in the encoding period, nearly returned to baseline during delay, and peaked once again at retrieval. As shown in Figure 4A, the main effect of activity across loads was significant during the early encoding, late encoding, and retrieval periods, but not for the delay. While it appeared that FFA simply activated when faces were present in the visual field, the load effects revealed a more complex pattern of activity. Stratified by mnemonic load, activity during both the encoding and delay periods increased with face load (Figure 3). Unlike the step function suggested in the PFC, activity in FFA appeared to increase monotonically with memory load. FFA load-related linear increases were statistically significant during encoding and delay periods (Figure 4B).

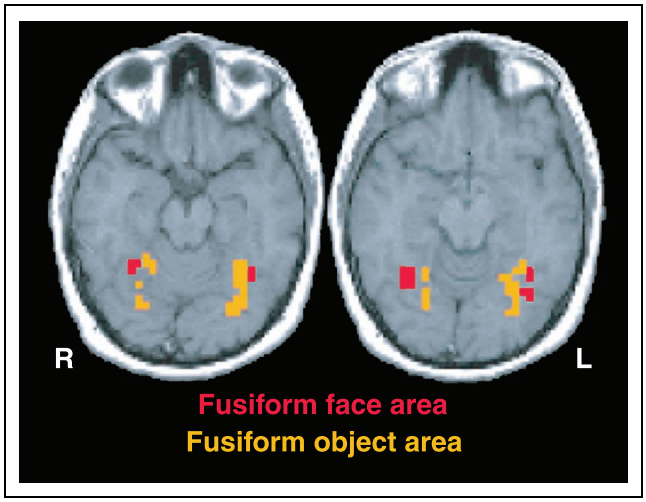

Figure 2. Representative subject illustrating the location of the FFA (red) and FOA (yellow) ROIs. The FFA was generally smaller in size and lateral in location relative to the FOA. The data from this figure can be viewed interactively on-line at The fMRI Data Center (www.fmridc.org), Accession Number 2-2003-113HT.

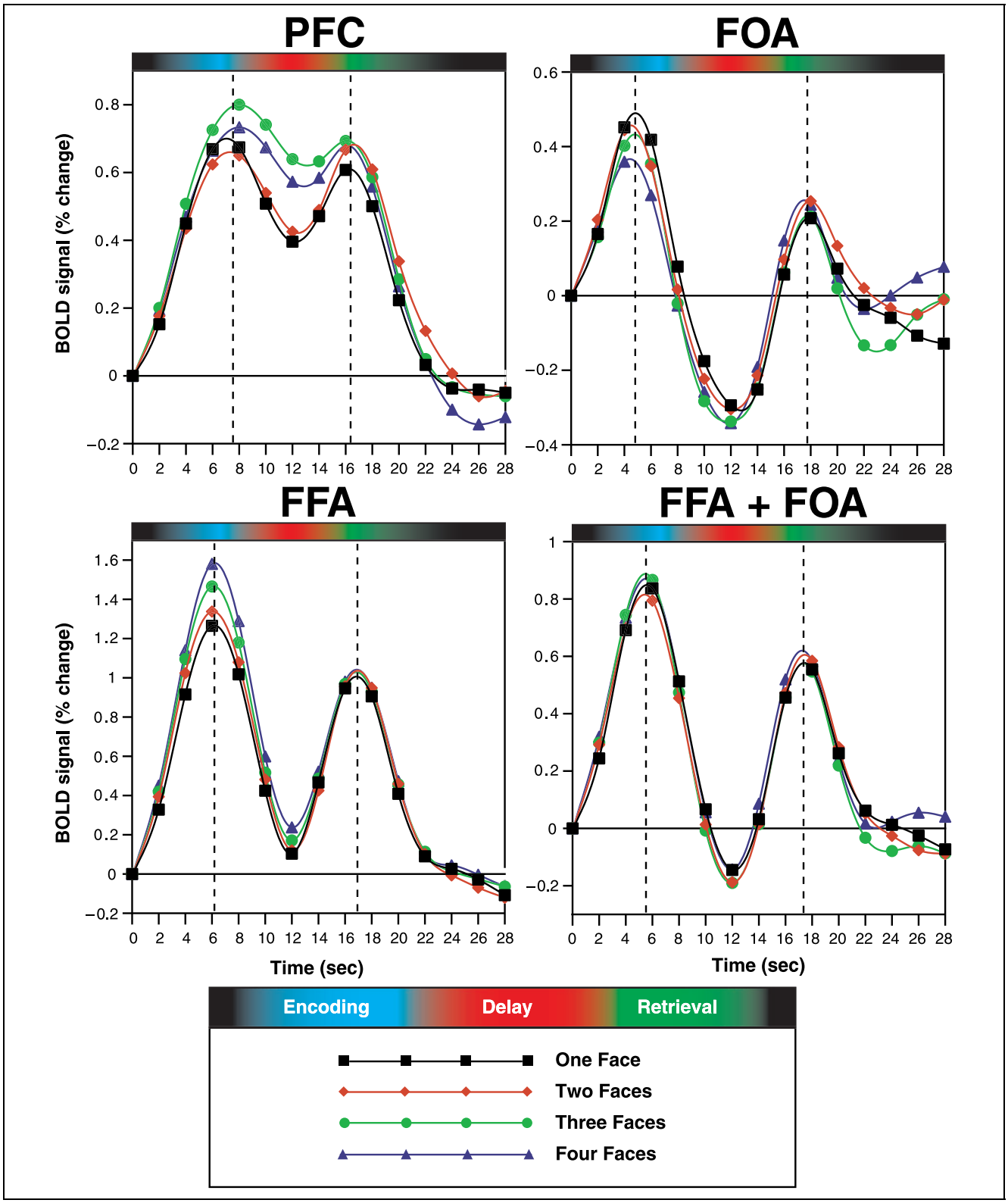

Figure 3. These time series reflect the average percent change in BOLD signal over the course of a behavioral trial for: PFC, FFA, FOA, and FFA and FOA combined. For each mnemonic load and ROI, percent change of BOLD signal was averaged (1) across trials of the same mnemonic load, (2) within the ROI, and (3) across all subjects. Because the BOLD signal lags neural activity by roughly 4–6 sec, the spectrum at the top of each graph shows a temporal reference for where to expect peak activity during encoding (blue), delay (red), and retrieval (green) periods. The vertical dotted lines mark peak activities during the encoding and retrieval periods, averaged across mnemonic load.

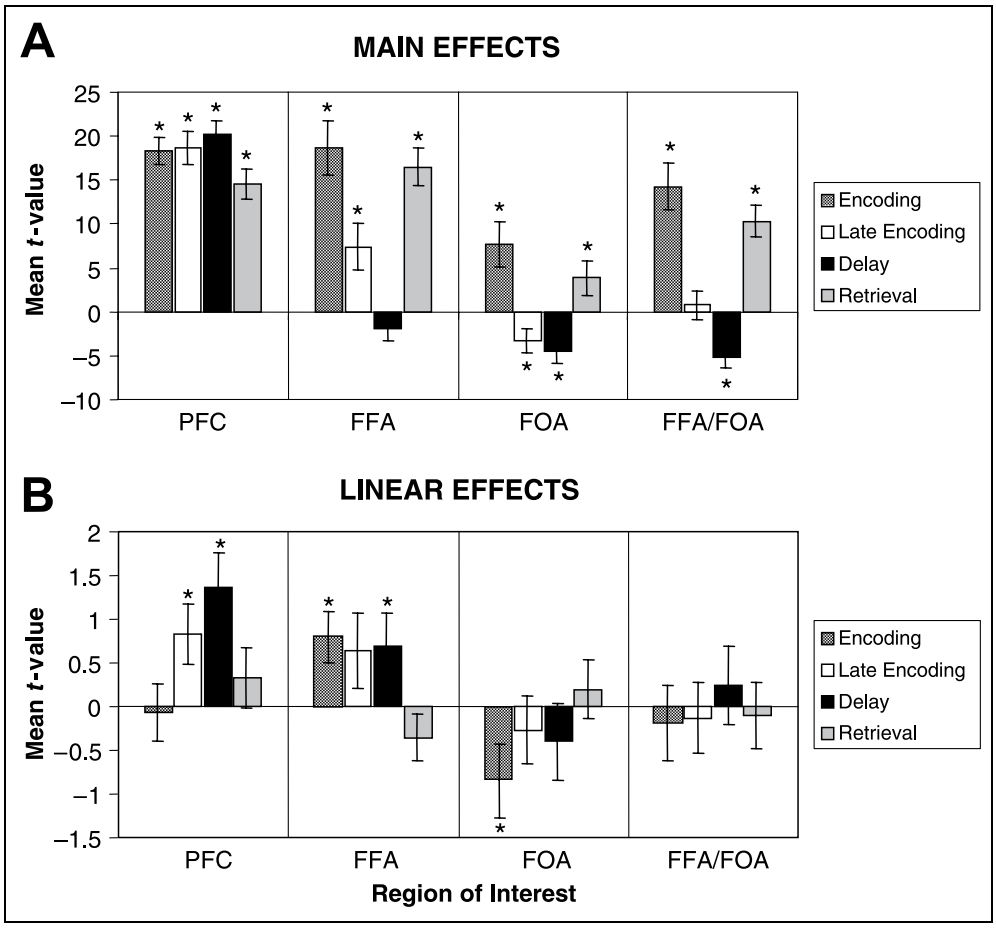

Figure 4. Main and linear effects of the regression analyses across subjects, separated by ROI (PFC, FFA, FOA, and FFA/FOA) and trial period (early encoding, late encoding, delay, and retrieval). (A) Main effects indicate BOLD signal compared against the baseline. (B) Linear effects describe how well increasing mnemonic load describes changes in BOLD signal. The *x* axis depicts ROIs further divided by trial period. The *y* axis depicts *t* values for the contrast describing the relevant effect (main or linear). The bars show the mean and standard error of the *t* values measured in individual subjects ($N = 10$). Regions and trial periods showing significant effects ($p < .05$) are indicated with an asterisk.

In contrast to both the PFC and FFA, activity in FOA did not persist throughout the trial (Figure 3). For all mnemonic loads, FOA activity peaked at encoding, traveled well below baseline during the delay period, and peaked again at retrieval. The main effect of activity across loads was significantly positive at early encoding and retrieval, but significantly negative during the late encoding and delay periods (Figure 4A). When stratified by load, activity at the encoding peak decreased with the number of faces presented (Figure 3). Linear decreases with mnemonic load were only statistically significant during the early encoding period (Figure 4B). The negative linear effects at early encoding probably result from decreases in the number of scrambled faces that appear with increased intact face load. Assuming a scrambled face is processed more as complex object than a face, such decreases would be expected in an object-selective area.

The analyses presented in Figure 4B demonstrate a linear component to the activation found in several different regions and trial periods. Although significant linear effects were found, we did not have a priori prediction that parametric manipulations would produce truly linear effects in BOLD signal. Processes mathematically described by step functions or logarithmic functions could also show significant linear components. Figure 5 presents the data in a format that allows a more descriptive evaluation of the parametric effects. Bold lines indicate regions and trial periods with significant linear effects from the previous analysis. The FFA effects during encoding and delay result from a nearly monotonic increase in the data points with mnemonic load. In contrast, the PFC effects during the late encoding and early delay periods appear to result from a step function between the two- and three-face loads.

Imaging Data: Time-to-Peak Activity at Encoding and Retrieval Periods

Due to regional variability in the HRF, interpreting absolute differences in time-to-peak activity between anatomic regions is not possible without an explicit representation of the HRF for each region (Miezin, Maccotta, Ollinger, Petersen, & Buckner, 2000). In contrast, we can interpret relative changes in these absolute differences with the assumption that the transform between neural activity and BOLD response remains constant within an anatomic region. In all ROIs, peaks of activity were observed 4–8 sec following the onset of the encoding and retrieval periods (vertical dotted lines in Figure 3). Calculating the time-to-peak activity following the onset of either encoding or retrieval (Figure 6;

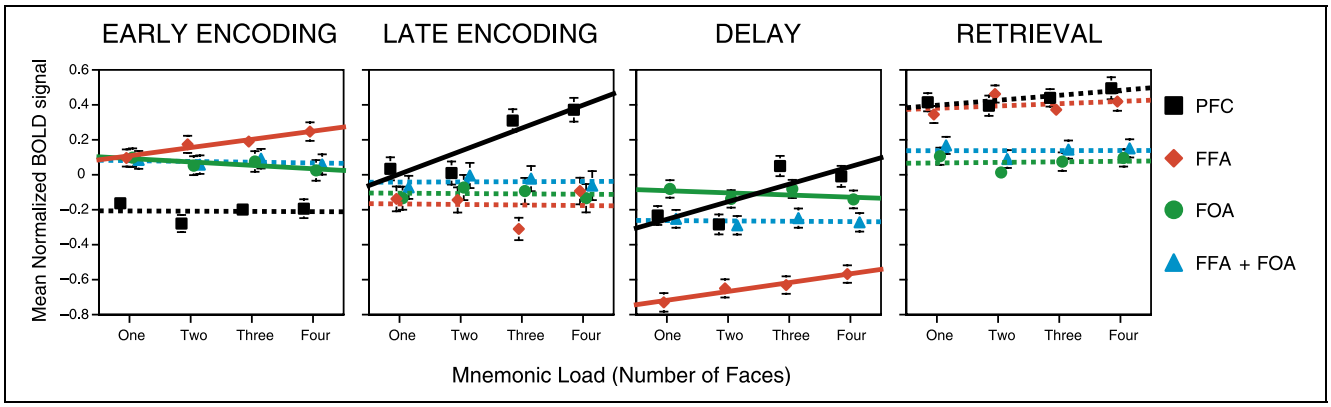

Figure 5. Plot of mnemonic load against an estimate of the BOLD signal measured from all subjects. This estimate was derived for every trial period of every behavioral trial (details described in the Methods). The estimates were *z*-normalized within each subject to allow all subjects to be combined on the composite graph. Data from all subjects ($N = 10$) were then separated into groups by trial period, ROI, and mnemonic load. The points in the figure represent the mean and standard error of each group. The lines indicate the simple regression of the grouped data onto a numeric index of mnemonic load. Solid lines indicate regions and trial periods where the slope of the linear fit was statistically significant ($p < .05$).

Table 1) revealed that FFA activity during the encoding period peaked 1262 msec prior to the PFC encoding peak. In contrast, FFA activity during the retrieval period peaked 544 msec after the PFC retrieval peak. This interaction between trial period (encoding or retrieval) and ROI (FFA or PFC) was significant, $F(1,36) = 8.61$, $p = .05$. At encoding, PFC showed a trend toward later time-to-peak activity with increased mnemonic load, although this trend did not reach statistical significance. No such trend was observed in the FFA.

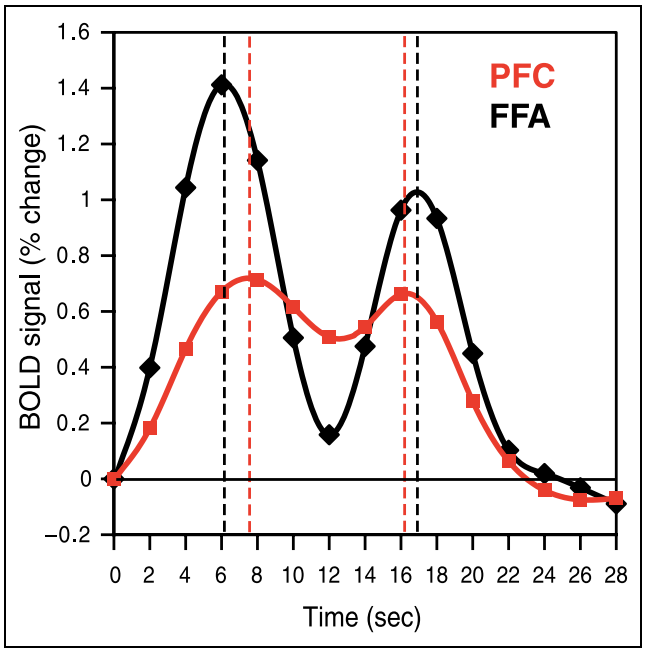

Figure 6. Trial-averaged time series plots (solid curves) from FFA (black) and PFC (red), combined across all four mnemonic loads. The first pair of vertical bars (dashed lines) indicates the time point for the encoding peaks of the two curves. The second pair of vertical bars marks the time for the retrieval peaks of the two curves. The FFA peak precedes the PFC peak during the encoding period, and this order reverses at the retrieval period.

Imaging Data: Working Memory Contrasts within Anatomically Defined ROIs

Random effects analyses were used to compare data across individual subjects after normalization to a standard anatomic space. These analyses focused on anatomically defined portions of the ventral temporal lobe and PFC. As in the functional ROI analyses, each region and trial period were examined for (1) main effects compared against baseline and (2) linear effects of memory load. Tests for main effects across all task periods showed that memory encoding and retrieval recruit overlapping but distinct regions spread widely throughout the ventral temporal lobe and PFC (Figure 7). Activation in both the

Table 1. Time-to-Peak Encoding and Retrieval Activity

ROI	*Number of Faces*	*Time-to-Peak Encoding Activity (msec)*	*Time-to-Peak Retrieval Activity (msec)*
FFA	One	6250	4950
	Two	6225	5075
	Three	6175	4825
	Four	6225	4850
	Mean	6219	4925
PFC	One	7025	4375
	Two	7225	4425
	Three	7825	4350
	Four	7850	4375
	Mean	7481	4381

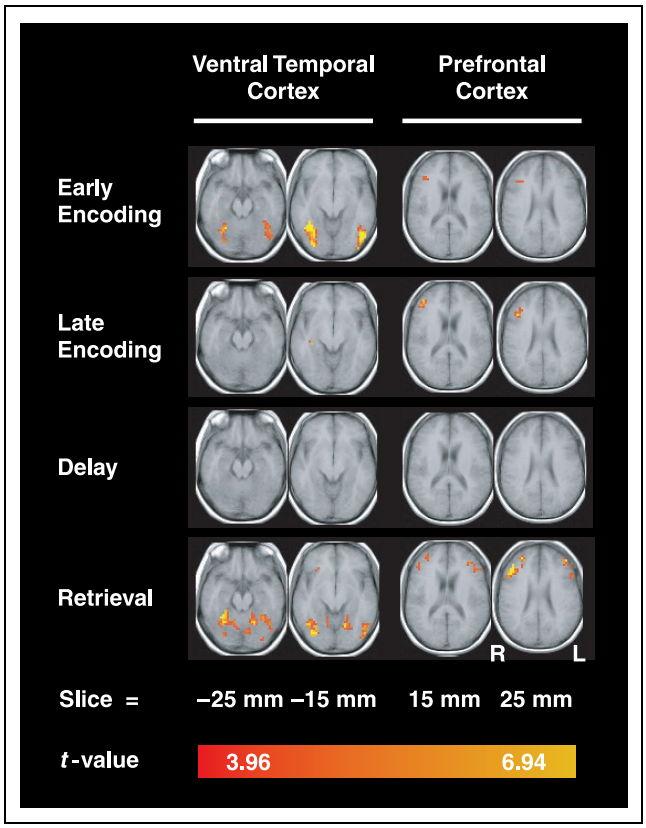

Figure 7. Random effects analyses across all subjects, testing for activity in each separate trial period as compared against baseline. Analyses focused on the anatomically defined ventral temporal cortex and PFC. Two representative slices are shown from each ROI. A spectrum of t values is provided to quantify the statistical significance of contrasts during each trial period. The data from this figure can be viewed interactively on-line at The fMRI Data Center (www.fmridc.org), Accession Number 2-2003-113HT.

ventral temporal lobe and PFC was notably absent during the delay period, despite these areas showing delay period activity in our ROI analyses. Evaluation of individual subject data within native anatomic space revealed an explanation for this result. Figure 8 shows the main effect of delay contrasted against baseline in PFC slices from all 10 subjects. Each subject clearly has delay period activation (warm colors) in some portion of

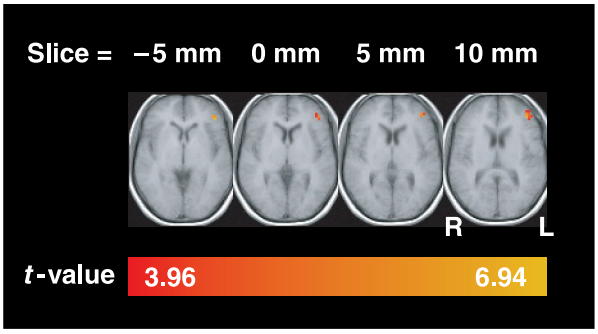

Figure 9. Random effects analysis of PFC regions showing delay period activity that increased linearly with increased memory load. A spectrum of t values is provided to quantify the statistical significance of the contrast. The coordinates of this activation based on the Montreal Neurological Institute template brain are $x = 45$, $y = 45$, $z = 10$. The data from this figure can be viewed interactively on-line at The fMRI Data Center (www.fmridc.org), Accession Number 2-2003-113HT.

PFC, but activation is not consistently located in any particular region of PFC across subjects. This heterogeneity of spatial location of the delay period activity resulted in no consistent finding in normalized data. During the delay period, there were also deactivations (cold colors) throughout the PFC in all subjects.

Increases in activity with increased memory load were observed during the delay period within the left middle frontal gyrus (Figure 9), but not in the ventral temporal cortex. Tests for linear effects in trial periods other than the delay revealed no significantly positive effects. Given the ROI results demonstrating positive correlations with memory load in FFA during encoding and delay, this null finding in the spatially normalized data suggests that the spatial location of load effects within the fusiform gyrus is not consistent across subjects.

DISCUSSION

In the present study, we parametrically varied the mnemonic load of a face delayed recognition task to test the different roles of the PFC and the FFA in face working memory. Our results revealed that activity during the

Figure 8. PFC activity during the delay period in individual subjects. Three representative slices (inferior, middle, and superior) are shown for each of the ten subjects. Warm colors indicate voxels with significant activation; cold colors indicate voxels with significant deactivation. The data from this figure can be viewed interactively on-line at The fMRI Data Center (www.fmridc.org), Accession Number 2-2003-113HT.

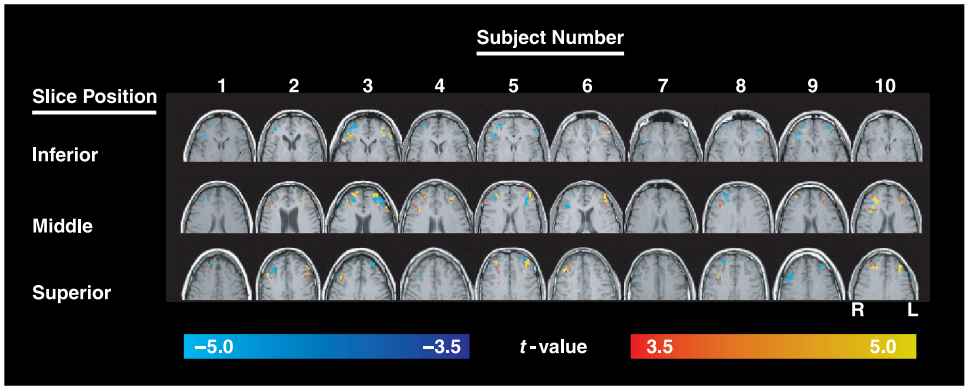

retention period increased parametrically with memory load in both the PFC and FFA. Furthermore, differences in the timing of fMRI signal during the cue and probe period of the task suggested a shift in the flow of information between these two regions associated with encoding and retrieval. We describe these findings in more detail and consider their implications below.

Despite differences in method and species of study, there are striking parallels between the present fMRI results and monkey neurophysiology studies reporting single-unit activity patterns within frontal and temporal cortex. The time course of fMRI signal within the human FFA parallels that of stimulus-specific IT neurons exposed to a preferred stimulus: rising sharply at the time the stimulus is encoded, hovering above baseline during maintenance of the stimulus across a delay interval, and reactivating when the memory trace must be retrieved to initiate a decision. In addition, the time course of fMRI signal within the human FOA mirrors stimulus-specific IT neurons viewing a nonpreferred stimulus: activating weakly at encoding, not activating or deactivating below baseline during the delay, and weakly reactivating at retrieval (e.g., Nakamura & Kubota, 1995; Chelazzi, Miller, Duncan, & Desimone, 1993; Miyashita & Chang, 1988; Fuster & Jervey, 1982). Finally, the time course of fMRI signal within the human PFC generally parallels monkey PFC neurons: activating robustly at encoding, maintaining a plateau during the delay, and strongly reactivating at retrieval (for a review, see Funahashi & Takeda, 2002).

In this study, we sought to isolate maintenance processes by varying memory load, and to identify the neural correlates of maintenance by identifying regions that exhibited a significant relationship between imaging signal and increasing load. The parametric effects of memory load observed in this study have no direct correlate in the existing monkey literature. In monkeys, single PFC neurons are known to code stimulus features that vary parametrically (Romo, Brody, Hernandez, & Lemus, 1999), but identifying a distributed neural network in maintaining increasing numbers of stimuli with single-unit recording is difficult. Simultaneous multiple neuron recording has the potential to address this issue in monkeys (Nicolelis, Ghazanfar, Faggin, Votaw, & Oliveira, 1997), but working memory studies of this nature have not been attempted. Nonetheless, the present fMRI results confirm logical extensions of many ideas proposed in the existing single-unit literature monkey physiological literature.

In our study, we found that lateral PFC exhibited a load-related increase in activity during encoding and delay periods of the face delayed recognition task. Delay period load effects provide further support for a role of PFC in maintenance processes consistent with numerous other human imaging studies that observed delay period activity in match-to-sample tasks that did not vary load (e.g., D'Esposito, Postle, Ballard, & Lease, 1999; Zarahn, Aguirre, & D'Esposito, 1999; Courtney, Ungerleider, Keil, & Haxby, 1997). Although the location of delay period activity within PFC varied between subjects in our study, the PFC region that consistently showed load-related increases across subjects is consistent with other human (Sala, Rama, & Courtney, 2003; Rama, Sala, Gillen, Pekar, & Courtney, 2001; Courtney et al., 1997; Courtney, Petit, Maisog, Ungerleider, & Haxby, 1998) and monkey (Scalaidhe, Wilson, & Goldman-Rakic, 1999b) studies of face working memory. Another empirical observation in our study worth noting is the finding that delay activity in the PFC ROI exhibited a step function in the transition from remembering two faces to remembering three faces. At the outset, we predicted a monotonic increase in PFC activity with increasing memory load. Recent studies have suggested that the PFC, in addition to having a mnemonic role, might also function in chunking and compressing information as working memory storage approaches its limited capacity (Bor, Duncan, Wiseman, & Owen, 2003; Rypma, Prabhakaran, Desmond, Glover, & Gabrieli, 1999). Thus, we speculate that the step function represents recruitment of PFC to perform additional cognitive processes necessary at higher memory loads.

Increases in FFA activity with the number of faces presented at encoding support the idea of faces being coded by distinct (and probably overlapping) populations of neurons (Perrett, Rolls, & Caan, 1982). Likewise, reductions in FOA activity with the number of encoded faces reveal that complex, nonface stimuli are coded by distinct populations of neurons anatomically segregated from those coding faces (Gross, Rocha-Miranda, & Bender, 1972). Parametric modulation of FFA delay activity by mnemonic load supports the idea that a component of the memory trace is represented in stimulus-specific temporal cortex during the maintenance period. This finding is consistent with previous visual working memory studies in monkeys that have found sustained activity during the delay period of visual working memory tasks within temporal cortex (Nakamura & Kubota, 1995; Miyashita & Chang, 1988; Fuster & Jervey, 1982). However, if activity in human FFA reflects working memory maintenance processes, then why did we fail to find significant differences in the magnitude of overall delay period activity relative to the intertrial interval? One possibility is that the FFA likely represents an inhomogeneous region of cortex, containing both face-selective and non-face-selective neurons (Haxby et al., 2001). If the activation of face-selective neurons during active maintenance occurs simultaneously with the inhibition of non-face-selective neurons within the FFA, then the averaged BOLD signal resulting from this competition will be less than in a region such as the PFC, which is not as stimulus-specific. Thus, face-selective neurons could be intensely active in such a region despite an overall low BOLD signal (Avidan, Hasson, Hendler, Zohary, & Malach, 2002). Also, given

this hypothesis, one would predict the BOLD signal of a region containing a smaller proportion of face-selective neurons (e.g., FOA) to show more inhibition, which was what we observed empirically within the FOA.

Previous studies have yielded conflicting results regarding whether face working memory is associated with sustained activity in visual association cortex. For example, two recent face working memory studies in humans have reported significant activity during a memory delay in fusiform gyrus (Sala et al., 2003; Rama et al., 2001). In contrast, another fMRI study that manipulated memory load for faces found no evidence to suggest delay period extrastriate visual cortical activity (Jha & McCarthy, 2000). One potentially substantive difference between our study and these studies of face working memory is the manner in which extrastriate activity was measured. In our study, we functionally defined face-sensitive regions of extrastriate cortex using a separate face perception task, whereas Jha and McCarthy (2000) examined activity within an anatomically defined fusiform gyrus ROI. It is likely that the fusiform ROI defined by Jha and McCarthy (2000) included not only face-sensitive regions, but also regions showing different patterns of category specificity (Haxby et al., 2001). In the other studies (Sala et al., 2003; Rama et al., 2001), it is not clear if the visual association cortical region exhibiting sustained delay period activity was the FFA because a separate face perception task was not performed. The load-dependent memory effects that we obtained were specific to the FFA, because a contrasting pattern of activity was seen in the FOA. Also, we found that combining the data from these regions into a composite FFA/FOA ROI eliminated many of the significant effects found in the individual ROIs. Thus, our results suggest that working memory maintenance does not modulate activity throughout the extrastriate cortex, but that this modulation enhances activity only in stimulus-selective cortical areas.

Another salient difference between our study and the Jha and McCarthy (2000) study was in the methods used to statistically characterize delay period activity. In our study, we used a multiple regression-based approach (Postle, Zarahn, & D'Esposito, 2000; Courtney et al., 1997; Zarahn, Aguirre, & D'Esposito, 1997b) to deconvolve HRFs attributable to different trial components (i.e., encoding, delay, and retrieval periods). In contrast, Jha and McCarty statistically evaluated differences in percent signal change measured at specific points in the trial-averaged time courses. Thus, the method used by Jha and McCarthy makes no assumptions about the shape of the HRF associated with different trial components, whereas our method explicitly accounts for intersubject variability. For example, in a study with delay lengths comparable to the present study, one might expect the negative postpeak undershoot of an encoding-period response to overlap with positive responses associated with delay period activity. Analyses of specific points in averaged time courses across subjects would fail to take such effects into account, resulting in inadequate sensitivity to detect subtle but reliable delay period activity changes. Jha and McCarthy avoided this difficulty to some extent by using trials with very long (e.g., 15 and 24 sec) delays. However, it is unclear whether subjects continue to maintain rehearsal to bridge such long delays or whether they employ qualitatively different strategies than those employed at short delays.

The analysis of the temporal dynamics of the BOLD signal within PFC and FFA may provide information about the interaction between these regions during our face working memory task. Empirical investigations of the nature of the BOLD signal indicate that time-to-peak activity shows a strong correlation with time to onset (Miezin et al., 2000), which correlates well with time to onset of neural activity (Menon, Luknowsky, & Gati, 1998). Thus, latency differences in peak responses between ROIs and particular trial periods may be meaningful.

In our study, at the time of presentation of faces to be remembered, the activity in PFC lagged behind the visual association area encoding the behaviorally relevant stimulus—the FFA. This PFC activity at encoding, coupled with parametric increases significant through the delay, supports the idea that PFC participates in more elaborative encoding of stimuli and maintenance of behavioral relevance when stimuli are not present in the environment (Desimone, 1996). In contrast, at the time of presentation of the probe, which requires a recognition decision and a response, peak activity within PFC preceded that observed in the FFA. This finding supports the idea that the PFC may also initiate retrieval and decision processes (Schall, 2001). Overall, there seems to be a context-dependent shift in the onset of PFC activity relative to FFA activity.

Based on timing information from single neuron recordings, the latency of neural activity to the presentation of face stimuli to monkeys is similar between IT and PFC (Scalaidhe, Wilson, & Goldman-Rakic, 1999a). In contrast, during delayed match-to-sample tasks, the presentation of the probe stimulus that represents a retrieval/decision period evokes PFC activity that precedes activity in IT (Miller, 1999; Rainer, Asaad, & Miller, 1998; Chelazzi et al., 1993). This shift in the onset of activity suggests a bottom-up flow of information at encoding, which changes to top-down flow at retrieval. Although the results from monkey neurophysiological studies occur on the order of tens of milliseconds, the present fMRI results, which are on a longer time scale, mirror the pattern of the shift between the onset of PFC versus IT during encoding and retrieval. Human ERP studies, which provide improved temporal resolution, may provide further support for this observed finding.

The present results guide us towards understanding the nature of visual working memory processes in both

humans and monkeys. Our fMRI data replicate a variety of single-unit phenomena supporting existing models of visual working memory originally derived from the monkey neurophysiological literature. These data suggest that the PFC establishes the behavioral relevance of a stimulus at encoding. To bridge a period between the encoding of relevant information and the time when such information must be acted upon, the PFC may bias activity in stimulus-specific temporal cortex in favor of a neuronal population that codes behaviorally relevant information. Finally, PFC may guide determination of the behavioral relevance of the probe stimulus. Although this model emphasizes the role of PFC in all facets of visual working memory, the present results additionally demonstrate a prominent role for other extrastriate cortical areas in visual working memory.

METHODS

Subjects

Ten right-handed subjects (age range 22–27 years) were recruited from the University of Pennsylvania Medical Center. All participants were screened against medical, neurological, and psychiatric illnesses, and also for use of prescription medications. All subjects gave written informed consent prior to participation in the study, as per the guidelines of the University of Pennsylvania Institutional Review Board. The day prior to the scan, subjects performed the behavioral task during a 30-min practice session.

Behavioral Task (Figure 1)

Each trial was composed of (1) a 4-sec encoding period, (2) an 8-sec delay, (3) a 2-sec retrieval period, and (4) a 16-sec intertrial interval. At encoding, the subject saw four serially presented images that were a mixture of gray-scale faces and gray-scale scrambled faces. Each image was on the screen for 1 sec, and subjects were asked to remember all of the intact faces. Sets of encoding stimuli contained between one and four intact faces, with the balance of the stimuli made up of scrambled faces. The order of face and scrambled face stimulus presentation was randomized so that the subjects did not know how many faces they would have to remember until the end of the encoding period. Faces were cropped to an ovoid shape so that peripheral face features (such as hair, ears, and neck) were not visible. During the delay period, subjects were instructed to fixate on a crosshair at the center of the screen. During the retrieval period, a single gray-scale face appeared and subjects were required to give a motor response indicating whether that face matched one of the faces presented at encoding. There were 15 volumes of images (later referred to as ''scans'') acquired per behavioral trial, 12 behavioral trials per run, and 8 runs per subject, for a total of 96 trials per subject. Trials were balanced for the number of faces and the number of match/nonmatch motor responses.

MRI Technique

Imaging was carried out on a 1.5 T SIGNA scanner (GE Medical Systems, Milwaukee, WI) equipped with a prototype fast gradient system for echoplanar imaging. A standard radiofrequency (RF) head coil was used with foam padding to comfortably restrict head motion. High-resolution sagittal and axial T1-weighted images were obtained in every subject. A gradient echo, echoplanar sequence (TR = 2000 msec, TE = 50 msec) was used to acquire data sensitive to the BOLD signal. Resolution was 3.75 × 3.75 mm in plane, and 5 mm between planes (21 axial slices were acquired). Twenty seconds of gradient and RF pulses preceded data acquisition to allow steady-state tissue magnetization. Subjects viewed a back-lit projection screen from within the magnet bore through a mirror mounted on the head coil.

Data Preparation

Off-line data processing was performed using the VoxBo analysis package (http://www.voxbo.org). Initial data preparation proceeded in the following steps: image reconstruction; sinc interpolation in time (to correct for the fMRI slice acquisition sequence); motion correction (six-parameter, rigid-body, least-squares alignment); slice-wise motion compensation (to remove spatially coherent signal changes via the application of a partial correlation method to each slice in time (Aguirre, Zarahn, & D'Esposito, 1998a; Zarahn et al., 1997b; Friston et al., 1995). The data were not spatially smoothed.

General Data Analysis

Because fMRI data are temporally autocorrelated under the null hypothesis (Zarahn et al., 1997b), statistical analyses were conducted within the framework of the modified general linear model (GLM) for serially correlated error terms (Worsley & Friston, 1995). In the convolution matrix (Worsley & Friston, 1995), a time-domain representation of the expected $1/f$ power structure (Zarahn, Aguirre, & D'Esposito, 1997b) and a notch filter that removed frequencies above the Nyquist frequency (0.25 Hz) and below 0.02 Hz (i.e., the portions of highest power in the noise spectrum) were placed.

Derivation of the Empirical HRF

The rationale for empirically deriving a hemodynamic response function (HRF) is described previously (Aguirre et al., 1998b). A HRF was derived from primary sensorimotor cortex in each subject in the following manner. Before performing the working memory task described above, each subject performed a task in which a central

white fixation cross changed briefly (130 msec) to a flickering checkerboard every 20 sec, cueing the subject to make a bilateral button press. Twenty such events occurred during the 400-sec run (200 scans). Due to the event-related nature of the behavioral paradigm, the data were not smoothed temporally. The data from this run were modeled by using a Fourier basis set of four sines and four cosines. A partial *F* test was used to evaluate the significance of activity in sensorimotor cortical voxels, and a HRF estimate was extracted from the suprathreshold voxels by averaging their time series. This empirical estimate of the HRF was used in subsequent analyses for each subject.

Identifying the FFA, FOA, and PFC

The FFA was identified in a separate experiment where subjects passively viewed 20-sec blocks of gray-scale faces and objects. A new image appeared every 2 sec and remained on the screen until the appearance of the next image. Subjects performed this task for two 400-sec runs (400 total scans). The GLM for this data set modeled the activity as 20-sec blocks of neural activity convolved by the subject's HRF. Due to the blocked nature of the paradigm, the data were smoothed temporally with the HRF in the course of the statistical analysis (Worsley & Friston, 1995). Based on individual sulcal and gyral anatomy, a ROI was drawn over the fusiform gyri for each subject. The FFA was subsequently defined as all voxels in the fusiform gyrus ROI showing statistically significant ($\alpha = .05$, Bonferroni corrected for number of statistical comparisons made within each ROI) activation in a contrast of faces against objects. A control area, which we call the FOA, was also defined within each fusiform gyrus ROI. The FOA was defined as all voxels in the fusiform gyrus showing a statistically significant ($\alpha = .05$, Bonferroni corrected for number of statistical comparisons made within each ROI) activation in a contrast of objects against faces. The PFC was defined based on the sulcal and gyral anatomy for each individual subject. Masks were drawn to include the middle frontal gyrus (Brodmann's areas 9/46) and inferior frontal gyrus (Brodmann's areas 44/45/47) based on a standard anatomic atlas (Talairach & Tournoux, 1988). The PFC ROI was then defined as the set of voxels within these gyri showing a significant ($\alpha = .05$, Bonferroni corrected for number of statistical comparisons made within each ROI) main effect across all trial periods and mnemonic loads during the face delayed recognition task.

Trial-Averaging the Face Working Memory Data (Results in Figure 3)

Trial averaging of the face working memory data generated waveforms reflecting the average change in fMRI signal over the course of a behavioral trial. First, the percent signal change in the fMRI time series was averaged across a ROI (PFC, FFA, FOA, or a combination of FFA/FOA). Next, timing data from the behavioral data were used to separate the mean fMRI signal into single behavioral trials. Then, the behavioral trials were segregated by mnemonic load (one, two, three, or four faces) and averaged within these load groups. For each subject, this procedure resulted in 16 waveforms (4 ROIs $\times$ 4 mnemonic loads). These waveforms were averaged across all subjects to produce 16 summary waveforms for the group. In each subject, percent signal change was calculated as the percent deviation from the mean fMRI signal measured across the subject's entire face working memory scanning session. After constructing each trial-averaged waveform, the percent change at time zero was subtracted from every point in the time series. This subtraction referenced the entire time series to the time point immediately prior to the start of the trial—presumably, a point where no task related should have been occurring.

Statistical Model of the Neural Activity (Results in Figure 4)

The GLM describes fMRI signal change as a series of amplitude-scaled and time-shifted covariates. Each covariate modeled a series of a brief neural events convolved by the subject's empirical HRF. Covariates were used to model early encoding, late encoding, delay, and retrieval periods for each level of mnemonic load (one, two, three, and four faces). Four trial periods with four load levels for each period gave a total of 16 covariates of interest. For each load, early encoding modeled the first two scans of a behavioral trial; late encoding modeled the third scan; delay modeled the fifth scan; and retrieval modeled the seventh scan. All other scans within a trial were considered as baseline. Additional nuisance covariates were included to model an intercept and trial-specific effects. Due to the event-related nature of the behavioral paradigm, the data were not smoothed temporally. Our inferential statistics were derived with a multiple regression where the data for each subject were modeled by linear combinations of the covariates of interest. Specifically, we examined the following: (1) main effects of trial period equally weighted across mnemonic load (contrast weights = [1,1,1,1]), and (2) linear effects within the trial period differentially weighted across loads (contrast weights = [−3,−1,1,3]). These analyses were conducted within each ROI. Contrasts to test for main effects within the PFC were adjusted to effectively give a weight of [1,1,1,1] while remaining orthogonal to the contrast used to define the ROI.

One concern in modeling activity during delay tasks is that neural activity limited to the encoding period might produce a hemodynamic response that extends into the subsequent delay period (due to the sluggishness of the hemodynamic response) leading to activity captured by the delay period covariate that is contaminated

by encoding period activity. However, we have demonstrated that spacing the onset of the delay period covariate at least 4 sec from the onset of cue and response covariates successfully identifies delay-specific activity, while activity earlier in the trial is modeled by the cue period covariate (Postle et al., 2000; Zarahn et al., 1997a).

Analysis for Linear Trends on Data Pooled Across Subjects (Results in Figure 4)

In this analysis, every scan except the baseline was modeled as an individual covariate of interest. Because we were still considering the same trial periods (early encoding, late encoding, delay, and retrieval), covariates were in the same temporal locations previously described. However, each scan was considered an event independent from other scans in a model that did not include nuisance covariates. The resulting model contained a total of 384 covariates of interest (4 trial loads × 24 trials of each load × 4 periods within a trial). Within the context of the modified GLM, each covariate was modeled as an individual event convolved by the subject's empirically derived HRF. A mean parameter estimate was obtained for each covariate, giving 24 parameter estimates per trial period per load per subject. Each parameter estimate is a scale factor that reflects changes in fMRI signal attributable to both task-specific effects and trial-specific confounds. To allow comparison of parameter estimates on the same scale across subjects, we z-normalized parameter estimates obtained from an ROI in each individual subject. Linear regression of all subjects' z-normalized parameter estimates for each trial period onto a numerical index of load (one, two, three, or four faces) gave a magnitude for any linear trend within that trial period and a statistical significance of that trend. This type of regression analysis allowed a separation of the trial-specific confounds from the parametric effects of varying mnemonic load within an ROI. Only correct trials were included in the analysis in an attempt to control for general effects of task difficulty, a subject that has been discussed previously (Druzgal & D'Esposito, 2001).

Time-to-Peak Time Series Analyses (Table 1)

In the trial-averaged responses from all ROIs, there were peaks of activity corresponding to the encoding and retrieval periods. Time-to-peak activity was measured as the time from the beginning of the trial period (encoding or retrieval) to the time where fMRI activity hit the next ''local'' maximum. Because data were only collected every 2 sec, we used two methods to identify ''local'' maxima. The first method used the actual data from individual subjects' ROIs to identify the time point (i.e., 2, 4, 6, 8 sec) where the maximum was reached in each subject. The times associated with the maximum were then averaged across subjects to produce a mean time to peak. The individual subjects' data were used for any references to statistical significance of the data. The second method of calculating time to peak used the composite data points shown in Figure 3. Interpolations between the data points were produced using the sinc interpolation routine from the VoxBo program. The interpolation simulated an effective sampling rate of 50 msec. The maxima measured directly from these curves represent the interpolated time to peak. The data in Table 1 represent the mean of the individual subjects' time to peak and interpolated time to peak.

Whole-Brain Random Effects Analyses (Results in Figure 7)

To perform random effects analyses, a whole-brain map of t values associated with a contrast was generated in each subject's native anatomical space. The t map for each subject was normalized to the Montreal Neurological Institute template brain found in SPM96b (www.fil.ion.ucl.ac.uk/spm) by applying a 12-parameter affine transformation with nonlinear deformations routine (Friston et al., 1995). Normalized t maps were then smoothed using a Gaussian smoothing kernel (7.5 mm full-width at half-maximum). For each voxel in the Talairach space (Talairach & Tournoux, 1988), the group of t values (one derived from each of the subjects) was one-way t tested for a significant difference from zero. The upper threshold for significance, $t(9) > 6.94$, was adjusted for multiple comparisons given the smoothness of the map to correct to a mapwise $p < .05$. The lower threshold for significance, $t(9) > 3.96$, was set to give a voxelwise $p < .001$. The result was a whole-brain Talairach-normalized map of voxels that showed the contrast of interest across subjects. These analyses were done to test for main and linear effects at encoding, late encoding, delay, and retrieval periods. In parallel with earlier analyses, we focused on the anatomically defined ventral temporal cortex and PFC.

Acknowledgments

This research was supported by NIH grants MH63901 and NS40813. We would like to thank Charan Ranganath for his helpful discussion of this work.

Reprint requests should be sent to Mark D'Esposito, University of California, 3210 Tolman Hall, Berkeley, CA 94720-1650, USA, or via e-mail: despo@socrates.berkeley.edu.

The data reported in this experiment have been deposited in The fMRI Data Center (http://www.fmridc.org). The accession number is 2-2003-113HT. Statistical contrast and results image maps are directly viewable via the fMRIDC web site.

REFERENCES

Aguirre, G. K., Zarahn, E., & D'Esposito, M. (1998a). The inferential impact of global signal covariates in functional neuroimaging analyses. *Neuroimage, 8,* 302–306.

Aguirre, G. K., Zarahn, E., & D'Esposito, M. (1998b). The variability of human, BOLD hemodynamic responses. *Neuroimage, 8,* 360–369.
Avidan, G., Hasson, U., Hendler, T., Zohary, E., & Malach, R. (2002). Analysis of the neuronal selectivity underlying low fMRI signals. *Current Biology, 12,* 964–972.
Bor, D., Duncan, J., Wiseman, R. J., & Owen, A. M. (2003). Encoding strategies dissociate prefrontal activity from working memory demand. *Neuron, 37,* 361–367.
Chelazzi, L., Miller, E. K., Duncan, J., & Desimone, R. (1993). A neural basis for visual search in inferior temporal cortex [see comments]. *Nature, 363,* 345–347.
Courtney, S. M., Petit, L., Maisog, J. M., Ungerleider, L. G., & Haxby, J. V. (1998). An area specialized for spatial working memory in human frontal cortex. *Science, 279,* 1347–1351.
Courtney, S. M., Ungerleider, L. G., Keil, K., & Haxby, J. V. (1997). Transient and sustained activity in a distributed neural system for human working memory [see comments]. *Nature, 386,* 608–611.
Desimone, R. (1996). Neural mechanisms for visual memory and their role in attention. *Proceedings of the National Academy of Sciences, U.S.A., 93,* 13494–13499.
D'Esposito, M., Aguirre, G. K., Zarahn, E., & Ballard, D. (1998). Functional MRI studies of spatial and non-spatial working memory. *Cognitive Brain Research, 7,* 1–13.
D'Esposito, M., Postle, B. R., Ballard, D., & Lease, J. (1999). Maintenance versus manipulation of information held in working memory: An event-related fMRI study. *Brain and Cognition, 41,* 66–86.
D'Esposito, M., Postle, B. R., & Rypma, B. (2000). Prefrontal cortical contributions to working memory: Evidence from event-related fMRI studies. *Experimental Brain Research, 133,* 3–11.
Druzgal, T. J., & D'Esposito, M. (2001). Activity in fusiform face area modulated as a function of working memory load. *Cognitive Brain Research, 10,* 355–364.
Friston, K. J., Ashburner, J., Frith, C. D., Poline, J.-B., Heather, J. D., & Frackowiak, R. S. J. (1995). Spatial registration and normalization of images. *Human Brain Mapping, 2,* 165–189.
Funahashi, S., & Takeda, K. (2002). Information processes in the primate prefrontal cortex in relation to working memory processes. *Reviews of Neuroscience, 13,* 313–345.
Fuster, J. M. (1997). *The prefrontal cortex: Anatomy, physiology, and neuropsychology of the frontal lobes* (3rd ed.). New York: Raven.
Fuster, J. M., & Bauer, R. (1974). Visual short-term memory deficit from hypothermia of frontal cortex. *Brain Research, 81,* 393–400.
Fuster, J. M., & Jervey, J. P. (1982). Neuronal firing in the inferotemporal cortex of the monkey in a visual memory task. *Journal of Neuroscience, 2,* 361–375.
Gross, C. G., Rocha-Miranda, C. E., & Bender, D. B. (1972). Visual properties of neurons in inferotemporal cortex of the Macaque. *Journal of Neurophysiology, 35,* 96–111.
Haxby, J. V., Gobbini, M. I., Furey, M. L., Ishai, A., Schouten, J. L., & Pietrini, P. (2001). Distributed and overlapping representations of faces and objects in ventral temporal cortex. *Science, 293,* 2425–2430.
Jha, A. P., & McCarthy, G. (2000). The influence of memory load upon delay-interval activity in a working-memory task: An event-related functional MRI study. *Journal of Cognitive Neuroscience, 12,* 90–105.
Kanwisher, N., McDermott, J., & Chun, M. M. (1997). The fusiform face area: A module in human extrastriate cortex specialized for face perception. *Journal of Neuroscience, 17,* 4302–4311.
Menon, R. S., Luknowsky, D. C., & Gati, J. S. (1998). Mental chronometry using latency-resolved functional MRI. *Proceedings of the National Academy of Sciences, U.S.A., 95,* 10902–10907.
Miezin, F. M., Maccotta, L., Ollinger, J. M., Petersen, S. E., & Buckner, R. L. (2000). Characterizing the hemodynamic response: Effects of presentation rate, sampling procedure, and the possibility of ordering brain activity based on relative timing. *Neuroimage, 11,* 735–759.
Miller, E. K. (1999). The prefrontal cortex: Complex neural properties for complex behavior. *Neuron, 22,* 15–17.
Miller, E. K., Erickson, C. A., & Desimone, R. (1996). Neural mechanisms of visual working memory in prefrontal cortex of the macaque. *Journal of Neuroscience, 16,* 5154–5167.
Miller, E. K., Li, L., & Desimone, R. (1993). Activity of neurons in anterior inferior temporal cortex during a short-term memory task. *Journal of Neuroscience, 13,* 1460–1478.
Miyashita, Y., & Chang, H. S. (1988). Neuronal correlate of pictorial short-term memory in the primate temporal cortex. *Nature, 331,* 68–70.
Nakamura, K., & Kubota, K. (1995). Mnemonic firing of neurons in the monkey temporal pole during a visual recognition memory task. *Journal of Neurophysiology, 74,* 162–178.
Nicolelis, M. A., Ghazanfar, A. A., Faggin, B. M., Votaw, S., & Oliveira, L. M. (1997). Reconstructing the engram: Simultaneous, multisite, many single neuron recordings. *Neuron, 18,* 529–537.
Perrett, D. I., Rolls, E. T., & Caan, W. (1982). Visual neurones responsive to faces in the monkey temporal cortex. *Experimental Brain Research, 47,* 329–342.
Postle, B. R., Zarahn, E., & D'Esposito, M. (2000). Using event-related fMRI to assess delay-period activity during performance of spatial and nonspatial working memory tasks. *Brain Research. Brain Research Protocols, 5,* 57–66.
Puce, A., Allison, T., Gore, J. C., & McCarthy, G. (1995). Face-sensitive regions in human extrastriate cortex studied by functional MRI. *Journal of Neurophysiology, 74,* 1192–1199.
Rainer, G., Asaad, W. F., & Miller, E. K. (1998). Selective representation of relevant information by neurons in the primate prefrontal cortex. *Nature, 393,* 577–579.
Rama, P., Sala, J. B., Gillen, J. S., Pekar, J. J., & Courtney, S. M. (2001). Dissociation of the neural systems for working memory maintenance of verbal and nonspatial visual information. *Cognitive Affective and Behavioral Neuroscience, 1,* 161–171.
Romo, R., Brody, C. D., Hernandez, A., & Lemus, L. (1999). Neuronal correlates of parametric working memory in the prefrontal cortex. *Nature, 399,* 470–473.
Rypma, B., Prabhakaran, V., Desmond, J. E., Glover, G. H., & Gabrieli, J. D. (1999). Load-dependent roles of frontal brain regions in the maintenance of working memory. *Neuroimage, 9,* 216–226.
Sala, J. B., Rama, P., & Courtney, S. M. (2003). Functional topography of a distributed neural system for spatial and nonspatial information maintenance in working memory. *Neuropsychologia, 41,* 341–356.
Scalaidhe, S. P., Wilson, F. A., & Goldman-Rakic, P. S. (1999a). Face-selective neurons during passive viewing and working memory performance of rhesus monkeys: Evidence for intrinsic specialization of neuronal coding. *Cerebral Cortex, 9,* 459–475.
Scalaidhe, S. P., Wilson, F. A., & Goldman-Rakic, P. S. (1999b). Face-selective neurons during passive viewing and working

memory performance of rhesus monkeys: Evidence for intrinsic specialization of neuronal coding. *Cerebral Cortex, 9,* 459–475.
Schall, J. D. (2001). Neural basis of deciding, choosing and acting. *Nature Reviews. Neuroscience, 2,* 33–42.
Talairach, J., & Tournoux, P. (1988). *Co-planar stereotactic atlas of the human brain.* New York: Thieme.
Worsley, K. J., & Friston, K. J. (1995). Analysis of fMRI time-series revisited—again [comment]. *Neuroimage, 2,* 173–181.
Zarahn, E., Aguirre, G., & D'Esposito, M. (1997a). A trial-based experimental design for fMRI. *Neuroimage, 6,* 122–138.
Zarahn, E., Aguirre, G. K., & D'Esposito, M. (1997b). Empirical analyses of BOLD fMRI statistics: I. Spatially unsmoothed data collected under null-hypothesis conditions. *Neuroimage, 5,* 179–197.
Zarahn, E., Aguirre, G. K., & D'Esposito, M. (1999). Temporal isolation of the neural correlates of spatial mnemonic processing with fMRI. *Brain Research. Cognitive Brain Research, 7,* 255–268.